

Physically based dynamic run-out modelling for quantitative debris flow risk assessment: a case study in Tresenda, northern Italy

Byron Quan Luna · Jan Blahut · Corrado Camera ·
Cees van Westen · Tiziana Apuani ·
Victor Jetten · Simone Sterlacchini

Received: 29 April 2013 / Accepted: 27 November 2013
© Springer-Verlag Berlin Heidelberg 2013

Abstract Quantitative landslide risk assessment requires information about the temporal, spatial and intensity probability of hazardous processes both regarding their initiation as well as their run-out. This is followed by an estimation of the physical consequences inflicted by the hazard, preferentially quantified in monetary values. For that purpose, deterministic hazard modelling has to be coupled with information about the value of the elements at risk and their vulnerability. Dynamic run-out models for debris flows are able to determine physical outputs (extension, depths, velocities, impact pressures) and to

determine the zones where the elements at risk can suffer an impact. These results can then be applied for vulnerability and risk calculations. Debris flow risk has been assessed in the area of Tresenda in the Valtellina Valley (Lombardy Region, northern Italy). Three quantitative hazard scenarios for different return periods were prepared using available rainfall and geotechnical data. The numerical model FLO-2D was applied for the simulation of the debris flow propagation. The modelled hazard scenarios were consequently overlaid with the elements at risk, represented as building footprints. The expected physical damage to the buildings was estimated using vulnerability functions based on flow depth and impact pressure. A qualitative correlation between physical vulnerability and human losses was also proposed. To assess the uncertainties inherent in the analysis, six risk curves were obtained based on the maximum, average and minimum values and direct economic losses to the buildings were estimated, in the range of 0.25–7.7 million €, depending on the hazard scenario and vulnerability curve used.

B. Quan Luna
Energy, Research and Innovation, Det Norske Veritas (DNV),
Veritasveien 1, 1363 Høvik, Norway

J. Blahut (✉)
Department of Engineering Geology, Institute of Rock Structure
and Mechanics, Academy of Sciences of the Czech Republic
(IRSM-ASCR), V Holešovičkách 41, 182 09 Prague, Czechia
e-mail: blahut@irms.cas.cz

C. Camera
Energy, Environment and Water Research Center, The Cyprus
Institute, 20 Konstantinou Kavafi, 2121 Aglantzia (Nicosia),
Cyprus

C. van Westen · V. Jetten
Faculty of Geoinformation Science and Earth Observation (ITC),
University of Twente, PO Box 6, 7500 AA Enschede,
The Netherlands

T. Apuani
Department of Earth Sciences “Ardito Desio”, Università degli
Studi di Milano, Via Mangiagalli 34, 20133 Milan, Italy

S. Sterlacchini
Institute for the Dynamic of Environmental Processes, National
Research Council (CNR-IDPA), Piazza della Scienza 1,
20126 Milan, Italy

Keywords Debris flow · FLO-2D · Run-out ·
Quantitative hazard and risk assessment · Vulnerability ·
Numerical modelling

Introduction

The analysis of hazard scenarios and their potential consequences is becoming an accepted and expected practice in risk reduction management (Glade et al. 2005). For this reason, landslide risk assessments have been a major research focus for the international community in recent times (Leroi et al. 2005; Dai et al. 2002; Cruden and Fell 1997). Several approaches have been applied in the past to

analyze landslide risk depending on the scope of the analysis; the scale of the study; the physical context; and social environment (van Westen et al. 2006). These approaches can be classified regarding the way they estimate the risk based on the level of quantification in: qualitative, semi-quantitative and quantitative methods (van Westen et al. 2006). Wong and Ko (2005) reviewed methodologies for landslide risk assessments for individual facilities focusing on the application of the methods in case histories.

Quantitative risk assessment (QRA) for landslides

Hazard magnitude and frequency and the vulnerability of the elements at risk were estimated for the analysis of hazard and risk scenarios and to assess the prospective losses. Complete quantitative landslide risk assessments still face many difficulties in expressing the temporal-spatial and intensity probability of hazard events, and the quantification of vulnerability (van Westen et al. 2006). These past attempts can be classified in terms of the applied methodology used for the analysis and the scale of the assessment. Castellanos (2008) used several methods for landslide risk assessment at different scales in Cuba. The applied scales were: (1) national scale (1:10,00,000), (2) provincial scale (1:1,00,000), (3) municipal scale (1:50,000), and (4) local scale (1:25,000). A quantitative method was used in the local scale where the hazard was assessed with dynamic run-out models based on rheological parameters and the vulnerability values were adopted based on flow depths and the conditions of the buildings. Economic risk values were computed for three different scenarios.

Only considering the initiation of the landslides at a regional scale, Remondo et al. (2008) and Zêzere et al. (2008) quantified risk using statistical analysis about past landslides and losses. Remondo et al. (2008) determined landslide risk in the Bajo Deba area (northern Spain) obtaining risk maps and tables of economic losses for a 50-year return period. The spatial landslide probability was assessed with a statistical landslide susceptibility model that related the past landslides and terrain parameters concerning slope instability. The temporal dimension of the hazard was based on the past landslide behaviour to calculate failure frequency for the next 50 years. For the vulnerability of the elements at risk, the ratio between the losses and the actual value of the elements affected was calculated. The risk was computed for each element considered in the analysis and indirect losses from the disruption of economic activities were assessed. Zêzere et al. (2008) determined landslide risk considering direct costs in the area north of Lisbon (Portugal). The hazard was assessed for three different types of slope movements based on statistical susceptibility analysis using past events

information and rainfall return period. This allowed development of different hazard scenarios based on the specific return period. The vulnerability was classified for the three landslide groups based on magnitude and damage levels. Direct costs for buildings and roads were calculated for each triggering scenario.

Jaiswal et al. (2010) applied a quantitative approach for landslide risk assessment to road and a railway line in the Nilgiri hills in southern India. Landslide events were catalogued initiating from cut slopes along the railway and road alignment and grouped into three magnitude classes based on the landslide type, volume, scar depth, run-out distance. Landslide probability was obtained using frequency–volume distributions. Hazard scenarios were generated using the three magnitude classes and six return periods. The assessment of the vulnerability of the road and railway line was based on damage records. Direct specific loss for the infrastructure (railway line and road), vehicles (trains, buses, lorries, cars and motorbikes) was expressed in monetary value, and direct specific loss of life was expressed in annual probability of death. Indirect specific loss derived from the traffic interruption was also evaluated.

Michael-Leiba et al. (2003) and Bell and Glade (2004) used the general angle of reach approach for estimating the run-out extension. Michael-Leiba et al. (2003) assessed landslide risk of Cairns, Australia. After a detailed mapping and characterization of the study area, the slope processes (landslide types and modes of occurrence) were defined. They collected information on the process rate from which landslide hazard may be assessed and spatial occurrence relations were made. Rainfall intensity–duration–frequency (IDF) curves were used to assess the mean recurrence intervals of rainfall triggering events. The total volumes of landslides triggered by three rainfall events and their run-out were estimated using an angle of reach approach. The vulnerability was assessed with historical data from past events in the Cairns area and the Australian landslide database. A risk map was created for resident people and buildings and the total risk for roads on hill slopes was assessed for a 10-year return period rainfall event.

Bell and Glade (2004) assessed landslide risk in NW-Iceland for debris flows and rock falls that focused on the risk to people. They analysed the hazards based on empirical and process modelling that resulted in specific run-out maps. The hazard zones were determined based on the recurrence interval of the respective processes. For the consequence analysis they defined and attributed vulnerability values to the elements at risk. The respective levels of vulnerability were defined by matrices based on a literature and the authors' findings during fieldwork. The factors considered were: vulnerability of people and

property; number of people; probability of temporal impact; probability of spatial impact; and probability of seasonal occurrence. Risk was calculated and portrayed in final risk maps as: object risk to people in buildings and individual risk to people in buildings.

Regarding the type of processes that are analysed (e.g. debris flows, slow moving landslides and rockfalls), several efforts have been done in the past to quantify the inflicted hazard and risk to the exposed elements. Different types of approaches have been applied which are dependent on the available information and the specific location of the assessment. In the case of rockfalls, Corominas and Mavrouli (2011) developed an application for a developed area by calculating the risk for buildings which are situated at the bottom of a rockfall prone slope and may be impacted by rock blocks. The frequency of the rockfall events was obtained from historical records and dendrochronology, while the probability of a rockfall reaching the developed area was estimated by trajectographic modelling. For every building, the risk was expressed in terms of the annual probability of loss and it is the sum, for all rockfall magnitudes, of the products of the rockfall frequency with the conditional probability of reaching the building with a certain kinetic energy sufficient to cause a specific state of damage and its associated vulnerability. An example of QRA for rockfalls was performed by Agliardi et al. (2009) where they study the case of Fiumelatte (Varenna, Italy), where a large rockfall in November 2004 resulted in two casualties, destruction of several buildings and damage to transportation corridors. The numerical model was calibrated by a back analysis of the 2004 event and then run for the whole area at risk by considering different scenarios. Finally, costs and benefits associated to different protection scenarios were estimated. Another example of a study case of rockfall hazard was carried out by Guzzetti et al. (2004), where they performed a risk assessment along a transportation corridor in the Nera Valley, Central Italy. They proposed a methodology based on the combined analysis of the recurrence of rockfall events, the frequency–volume statistics of rockfalls and the results of a physically based simulation models. Information on the location and type of rockfall defensive measures, including revetment nets, elastic fences, concrete walls, and artificial tunnels, was used to estimate the efficacy of the defensive structures and to determine the level of the residual rockfall risk along the roads. Recent work of Blahut et al. (2013) compared the modelling capabilities of two physically based models in the area of Hřensko and Dolní Žleb Municipalities in northwestern Czechia, an area of high rockfall hazard. They showed that the rockfall hazard modelling is highly depending on the local geomorphological conditions. The differences in hazard modelling were consequently reflected in assigning risk values to the exposed buildings.

For the case of landslides and slow mass movements, Cascini et al. (2005) discusses the improvement of urban planning and development by hazard and risk zoning which recognizes the efforts still required for quantifying zoning criteria and adapting them to landslides risk management necessities. As an example of an application, Malet et al. (2005) used a multi-disciplinary approach combining geomorphology, hydrology, geotechnics and rheology to model the initiation and run-out of the Super-Sauze landslide located in the Alpes-de-Haute-Provence, France. They concluded that slope failures induced by 25-year return period rainfall can trigger large debris flow events (30,000–50,000 m³) that can reach the alluvial fan and the elements at risk. Another study case was performed by Crosta et al. (2005) who carried out a cost-benefit analysis for the village of Bindo in the Valsassina valley (Central Pre-Alps, Italy). They built hazard scenarios with a method that coupled a stability analysis with a run-out assessment for different potential landslides. The different scenarios were compared with a scenario where no mitigation action was introduced. A cost-benefit analysis of each scenario was performed considering the direct effect on human life, houses, and lifelines.

For the rapid mass movement processes, Fuchs et al. (2008), provide a thorough introduction to the application of risk analysis for debris flow hazards that includes an overview of different methods for assessing risk. In a direct application for a debris flow case study, Hürlimann et al. (2006) used a multi-disciplinary approach for five torrent catchments in the Principality of Andorra. They produced a statistically based susceptibility map and created different scenarios to perform a run-out analysis with a one-dimensional numerical code. A final map was created based on a hazard matrix, which combined the intensity of the debris flow with its probability of occurrence. This map was used to assess the hazard mitigation and included some recommendations for hazard reduction. Another example for debris flow risk is the study carried out by Muir et al. (2006), where they presented a quantitative risk assessment to a site-specific natural terrain in Hong Kong. Various scenarios were generated with different source volumes and sets of rheological parameters for run-out assessment derived from the back analyses of natural terrain landslides. Individual risk was calculated as the summation of the product of the frequency of a flow affecting the facility and the vulnerability of the most vulnerable individual for each of the scenarios including the societal risk.

Numerical run-out modelling for landslide risk assessment is a relatively new research field. The problem in the application of such models is the difficulty in parameterization of the run-out models and the link between the modelling of initiation susceptibility (Chang et al. 2010) and the volume information for the subsequent run-out

analysis. Li et al. (2010) quantified the risk of cut-slope projects under construction using as example the Shuifu-Maliuwan Highway in the northeast of Yunnan Province in China. Finite element analyses determined the most dangerous landslide scenario among all construction steps. The slope failure probability was estimated using a Monte Carlo method to simulate the uncertainty and variability of soil and rock parameters. After identifying the failure surface and estimating the volume of the sliding mass with FLAC3D, the run-out behaviour was simulated with the PFC3D dynamic run-out model. Vulnerabilities of the exposed elements at risk were identified by values obtained from the literature. Landslide risk was assessed for three types of consequences: casualties, economic loss and lost time for clearing debris and reconstruction.

The above examples show the versatility and functionality of different approaches for quantitative landslide risk assessment. Depending on the availability and quality of the data, a QRA can be successfully applied to different scales, although it is most applicable to large scales (>1:10,000). A QRA can be carried out for different types of processes, different triggering events, environmental settings and for different objectives (e.g. cost-benefit analysis of risk reduction measures, emergency preparedness). One of the main advantages of a QRA is that it can be compared with other types of risk that can affect a community and because of its quantitative nature it can be communicated more comprehensibly to the policy and decision makers to be used for risk management strategies.

In this site-specific study, which is focusing on a village in the Italian Alps, hazard scenarios were prepared and risk was quantified as potential direct economic loss to buildings and individual risk to people. For the hazard scenario preparation, available meteorological and geotechnical data were used as inputs for a dynamic run-out modelling of possible debris flows. The hazard scenarios were validated using information about debris flow extent, from past events. The presented methodology is intended for an assessment of the bottom of the slopes as they are the most densely inhabited areas in mountain regions (Italian Alps), which can cause the largest damages. As reported in Blahut et al. (2012), most of the reported risk-related events in Alpine areas are located in the valley bottom. In addition, this can also valid for the transition part of debris flow track, as this section can be also properly modelled as the flow travels downslope. However, the proposed practice is not well applicable on the upper parts of the slope (detachment area) because not many buildings (assets/elements at risk) are present in the detachment areas—no particular need for QRA in that zones and the detachment areas are usually located in remote and/or inaccessible zones, which also make them limited for human development.

Study area

Tresenda village

The village of Tresenda, located in the municipality of Teglio (Fig. 1) in the Valtellina Valley in the Italian Central Alps, was selected as a case study. The valley has a U-shaped profile derived from Quaternary glacial activity and the axis of the valley is formed by the Adda River. The slopes are covered with colluvial and glacial sediments of variable thickness which are prone to debris flow initiation. Moreover, on south-facing slopes, dry stonewall terraces were built to allow for viticulture. These terraces were subject of several collapses in the past, caused by rapid increase of the water table after intense rainfall, which led to debris flow events, causing considerable damage. The study area is located in a very narrow part of the Valtellina Valley, and the main road is the only connection with the upstream tourist resorts and the rest of Lombardy Region.

Information from historical records, local chronicles and interviews with local people confirmed that the village was affected by debris flow events which caused significant losses in 1983, 2000 and 2003 (Blahut et al. 2012). Soil slips resulting in debris flows can be triggered on the steep slopes above Tresenda, as the soil thickness varies between 70 and 250 cm and the debris flow material consists of a mix of earth and boulders. The documented events indicate that debris flows crossed minor roads and impacted buildings in the Tresenda village, while running along main drainage lines (Cancelli and Nova 1985; Guzzetti et al. 1992). If a major event were to occur in the future, casualties and serious property damage can be expected as well as the interruption of the main road (S.S. 38) leading to high indirect losses.

Reconstruction of historical debris flow events in Tresenda

In May 1983, severe precipitation triggered more than 200 shallow landslides and debris flows in the Valtellina Valley. The rainfall station in Aprica measured a cumulated precipitation of 453 mm during the month, which corresponds to 34 % of the total annual precipitation (Guzzetti et al. 1992). In Teglio, three soil slips evolved into debris flows with lengths varying between 300 and 460 m and areas reaching 60,000 m². They occurred on 22nd and 23rd May on the slopes above the village of Valgella and Tresenda (Fig. 2), causing 14 casualties in Tresenda and 4 in the neighbouring village of Valgella (Cancelli and Nova 1985), and destroyed several buildings. The national road S.S. 38 was blocked and this isolated the upper part of the valley for few days.

Another intense rainfall event took place in the area in 2000, causing only one minor debris flow. A similar event

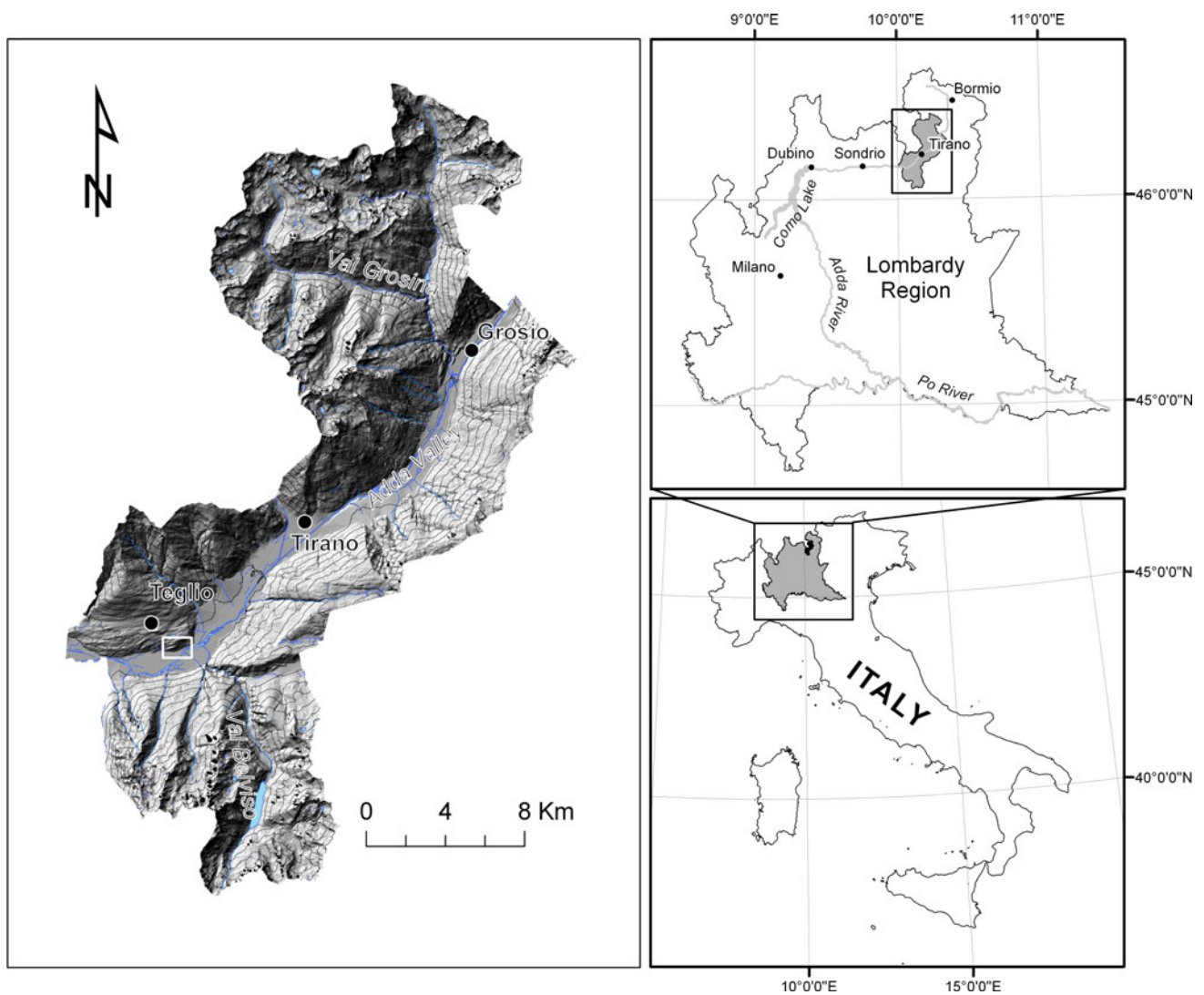


Fig. 1 Location of the Tresenda case study area shown as a *white rectangle*

as in 1983 happened on the same slope on 26th of November 2002 (Fig. 3), although producing less damage and no casualties. The flow remained confined and caused a minor flooding of the area close to the village due to an obstruction in the drainage channel (Di Trapani 2009, personal communication).

Preparation of hazard scenarios

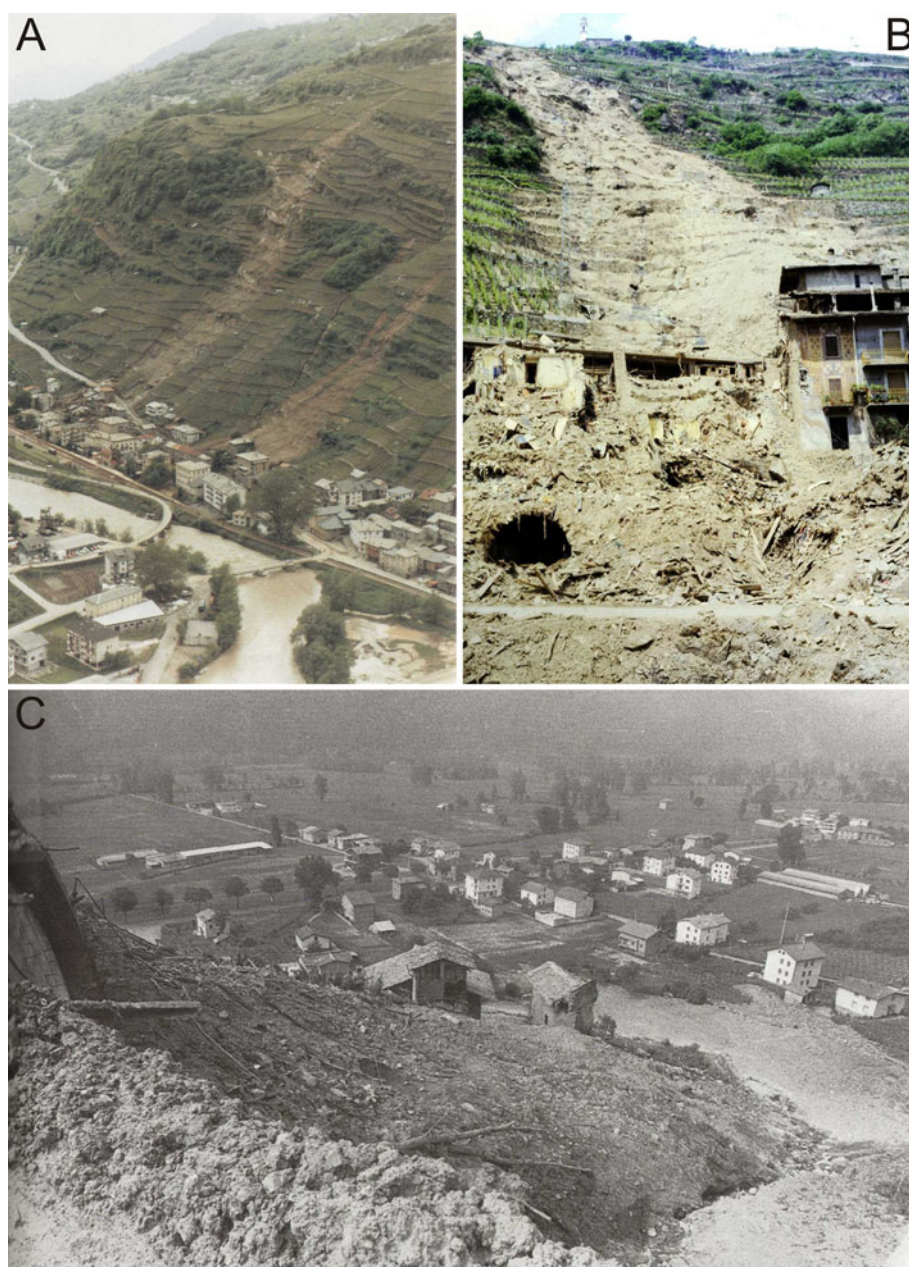
Methodological approach

Based on the historical events it was assumed that potential debris flows in the study area will be triggered in areas of steep slope and high surficial flow accumulation (Lara and Sepulveda 2010; Blahut et al. 2012). On the basis of a detailed field survey, DEM (digital elevation model) analysis and the generated debris flow susceptibility maps by

Blahut et al. (2010), three potential debris flow sources were selected (Fig. 3). These potential sources were modelled to assess the run-out intensity.

Several steps were implemented for the run-out modelling (Fig. 4): (1) detailed analysis of rainfall return periods and modelling of the rainfall-runoff processes for scenarios with different return periods: available hourly rainfall records were used to calculate 10, 50 and 100-year rainfall return periods. A 48-h rainfall, which may trigger a debris flow, was simulated in the study area and the time of exceedance of rainfall threshold was considered for the different return periods. The simulated rainfall was used to specify the time when rainfall threshold was exceeded and a debris flow triggered. The rainfall-runoff modelling allowed specifying nine input hydrographs for the three potential debris flow sources and three return periods. (2) analysis of the terrain features to determine the possible flow trajectories: taking as a starting point the debris flow

Fig. 2 **a, b** Photographs of two debris flows from 22nd and 23rd May 1983 in Tresenda. Photo: archive of CNR-IRPI, Torino. **c** Photograph of debris flow from 23rd May 1983 in Valgella. Photo source: Giacomelli (1987)



susceptibility maps produced by Blahut et al. (2010) and after a detailed analysis of the DEM (using slope and flow accumulation maps), the initiation areas were selected and delimited. These areas were later confirmed as susceptible for debris flow initiation after extensive fieldwork (including assessment of the state of dry-stone walls supporting the vineyards and survey of hydro-geological conditions—springs, wet areas). (3) laboratory tests of soil samples, estimation of the sediment concentration of the flow and determination of the debris flow rheology: soil samples were collected during fieldwork and analysed in a geotechnical laboratory. Samples were selected based on the criteria of the proximity location to the initiation and

run-out zones. Geotechnical parameters and particle size distribution for each sample were obtained and used to compute the volume of failed material. The calculated failed material was included as sediment concentration in the routed hydrographs. Rheological parameters (viscosity and yield stress) for the dynamic run-out model were also inferred based on the laboratory test results. (4) modelling of the run-out of the debris flows using the FLO-2D software: the debris flow scenarios were modelled with the 2-dimensional depth averaged FLO-2D software, using a quadratic rheological model that incorporates a Bingham shear stress as a function of sediment concentration and a combination of turbulent and dispersive stress components.

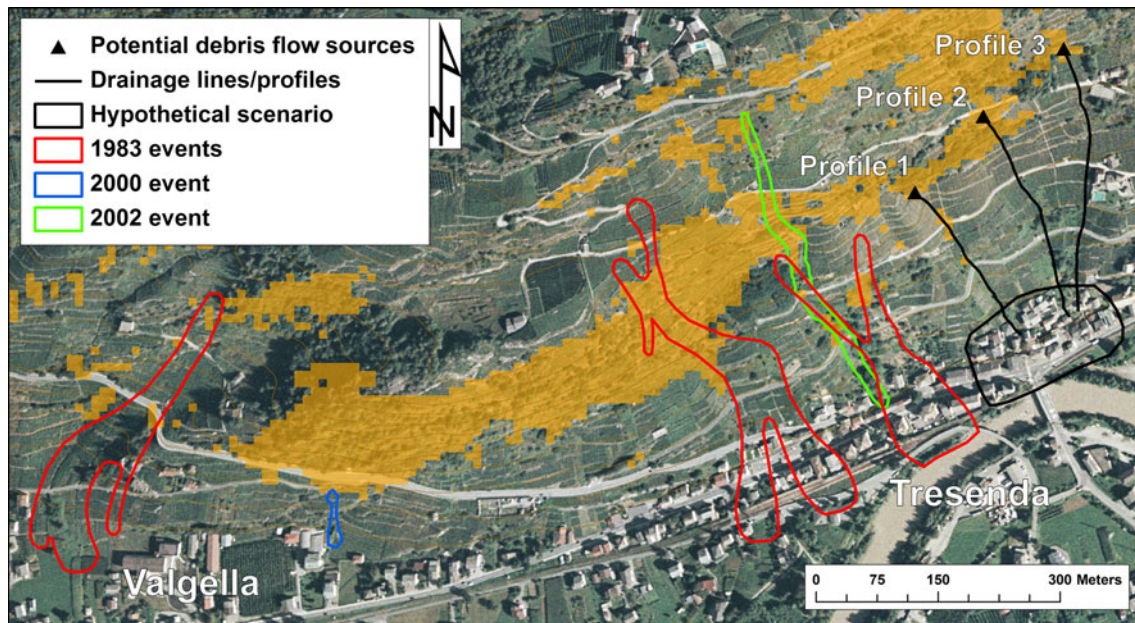


Fig. 3 Delimitation of the 1983, 2000 and 2002 debris flow past events. The area enclosed by the *orange colour* polygons comprises high and very high susceptible areas for debris flow initiation

generated by Blahut et al. (2010). The possible sources and drainage lines/profiles of new debris flows are shown and area of a hypothetical risk scenario is delimited in *black colour*

Rainfall modelling

Estimation of rainfall return periods

Hourly rainfall data for the period 1980–2009 from the range gauge at Castelvetro, located 3 km west from Tresenda, were analysed to calculate the return periods of rainfall events. To calculate the rainfall amounts for 10, 50 and 100-year return periods a Gumbel Extreme Value Type I distribution was used (Gumbel 2004; Khan et al. 2012). The results for the three return periods are summarised in Table 1.

Rainfall-runoff simulation and threshold

The debris flow resulting from a 48-h rainstorm was modelled using the FLO-2D code, because historical information (Guzzetti et al. 1992; Crosta et al. 2003; Di Trapani, personal communication) showed that past debris flow events in this area were usually caused by rainstorms with this duration. Since it is demonstrated that the rainfall distribution can affect instability in this area (Camera et al. 2012a) the rainfall during the 48-h rainstorm was discretized as a cumulative percentage of the total, based on the cumulative rainfall pattern of the 1983 event. The rainstorms were distributed spatially over a grid system and were calculated for all three rainfall return periods.

There are several rainfall thresholds for debris flow initiation available for the study area (Govi et al. 1984; Cancelli and Nova 1985; Ceriani et al. 1992; Agostoni et al. 1997; Luino et al. 2008). These rainfall thresholds show very similar results, except for the threshold by Luino et al. (2008), which shows much lower values than the others. Although it could be considered as being too conservative, it was used to recognize the minimum initiation time of the debris flows as a worst-case scenario. For a 10-year return period this threshold was exceeded after 22 h and 33 min of modelled rainfall. For a 50-year return period this threshold was reached after 18 h and 11 min of rainfall and for the 100-year return period after 17 h and 27 min (Fig. 5).

Laboratory analysis

Soil samples were collected between July 2009 and February 2010 along the slope uphill from Tresenda. Representative samples were selected based on the criteria of the proximity to the initiation and run-out zones. The materials are mixed loose deposits mostly composed of gravel (36 %) and sand (44 %) with a minor percentage of silt (19 %) and <1 % of clay. According to the ASTM Unified Soil Classification System, they are classified as GM (silty gravel with sand) or SM (silty sand with gravel), with a uniformity coefficient (CU) between 20 and 90. All samples were taken near the surface and they are relatively rich in organic matter (3.3–7.3 %). The bulk unit weight (γ_0)

Fig. 4 Flowchart of the debris flow hazard scenario modelling

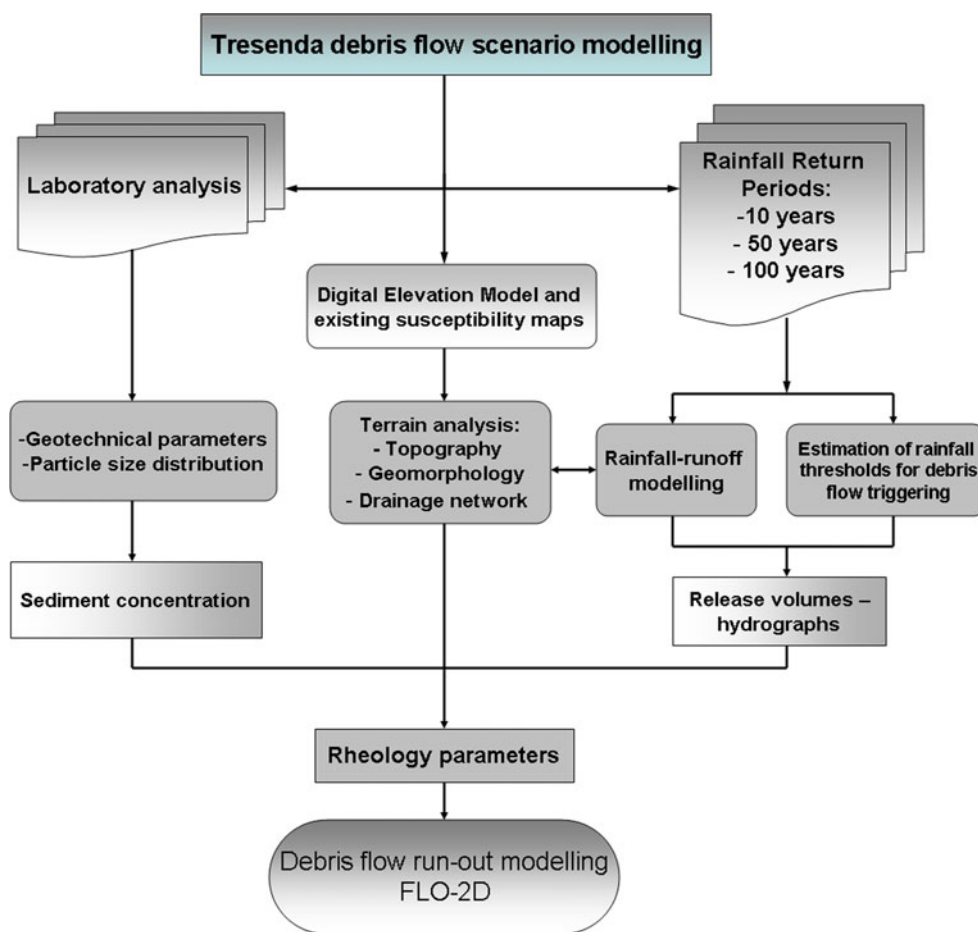


Table 1 Calculated precipitation for different return periods and rainfall duration

Return period	Precipitation (mm)		
	10 years	50 years	100 years
Duration (h)			
1	27 (±3)	36 (±4)	40 (±5)
2	40 (±5)	53 (±7)	59 (±8)
3	46 (±6)	61 (±8)	68 (±9)
6	61 (±8)	80 (±10)	89 (±11)
12	85 (±11)	113 (±14)	125 (±16)
24	112 (±14)	147 (±19)	162 (±21)
48	143 (±20)	192 (±26)	212 (±28)

was measured in place by the sand-cone method. The specific weight of the soil (G_s) equals to 27.2 kN/m^3 . Direct shear tests were performed to obtain the peak (c_p ; φ_p) and residual values (c_r ; φ_r) of the shear strength parameters. It was also possible to calculate porosity (n) and the sediment volumetric concentration (vc). A summary of the measured parameters is given in Table 2. These are in agreement with previous laboratory analysis of soils from nearby areas (Cancelli and Nova 1985; Crosta et al. 2003; Camera et al. 2012b).

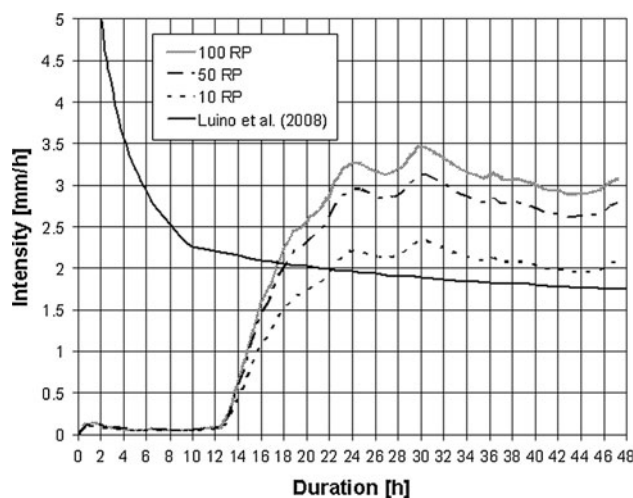


Fig. 5 Threshold exceedance of 10, 50 and 100-year return period rainfall intensities for the 48-h modelled rainfall

Debris flow modelling

The debris flow scenarios were modelled with the 2-dimensional depth averaged FLO-2D software. FLO-2D model uses a Eulerian formulation with a finite difference

Table 2 Summary of material characteristics obtained from in situ and laboratory tests

	C_p (kPa)	ϕ_p (°)	C_r (kPa)	ϕ_r (°)	N (m ³ /m ³)	V_c (m ³ /m ³)	γ_0 (kN/m ³)	CU
Max	18.50	36.50	17.00	36.50	0.52	0.60	16.10	90
Mean	10.70	33.80	12.95	30.45	0.46	0.54	14.95	45
min	3.40	27.50	6.60	26.30	0.40	0.48	13.80	20

numerical scheme that requires an input hydrograph as a boundary condition. FLO2-D uses a quadratic rheological model that incorporates a Bingham shear stress as a function of sediment concentration and a combination of turbulent and dispersive stress components based on a modified Manning n value (Eq.1). The internal stresses inside the flow are assumed to be isotropic.

$$S_f = \frac{\tau_y}{\gamma_m h} + \frac{K\eta V}{8\gamma_m h^2} + \frac{n_{td}^2 V^2}{h^{4/3}} \tag{1}$$

where S_f is the friction slope (equal to the shear stress divided by $\gamma_m h$); h is the flow depth; V is the depth-averaged velocity; τ_y is the resisting shear stress and η viscosity of the fluid, which are both a function of the sediment concentration by volume; γ_m is the specific weight of the fluid matrix; K is a dimensionless resistance parameter that equals 24 for laminar flow in smooth, wide, rectangular channels; and n_{td} is an empirically modified Manning n value that takes into account the inertial grain shear components of flow resistance (FLO-2D 2009).

The time when the rain storm exceeded the threshold was registered and discharge hydrographs with constant sediment concentration were produced using the rainfall-runoff component of FLO-2D software. Release volumes were calculated from the peak discharge of the hydrographs (Table 3, 4).

The rheological properties of the flow were estimated based on the results of the laboratory analysis using the mean values of the results. The final parameters used in the modelling were $\tau_y = 1,500$ Pa and $\eta = 2,800$ Pa. These parameters agree with the amount of sediment volumetric concentration of the flow and the particle size distribution (O’Brien and Julien 1988). The Manning n value that characterizes the roughness of the terrain was selected as $0.04 \text{ sm}^{1/3}$; this value corresponds to the lower boundary for open ground with no debris (FLO-2D 2009). The value of the friction angle was assumed for a residual state which was 30.5° and the specific weight of the soil used was equal to 27.2 kN/m^3 .

The results were validated for three different hazard scenarios using five historic events in the study area. Three debris flows from 1983, one from 2000 and one from 2002 were modelled using available rainfall data

Table 3 Peak discharge in cubic meters per second for the three profiles and return periods

	Peak discharge (m ³ /s)		
	10 years	50 years	100 years
Profile 1	4.8	11.4	13.4
Profile 2	4.2	11.2	13.3
Profile 3	5.1	12.1	14.1

Table 4 Release volumes in cubic meters for the three profiles and return periods

	Release volume (m ³)		
	10 years	50 years	100 years
Profile 1	390	1,160	1,420
Profile 2	330	1,140	1,410
Profile 3	425	1,250	1,520

from the Castelvetro rain gauge. Geotechnical parameters used for the modelling were than used for the hazard scenario preparation. Azzola and Tuia (1983) provided a detailed description of the debris flow event in 1983, which permits precise validation. Few hours before the triggering of the event, they described that the soil was saturated and later that the retaining dry-stone wall began to bulge at the toe for a length of 5 m, followed by its collapse over the downhill terrace. A muddy-debris flow resulted, which advanced initially with a relatively low velocity but gained velocity as it ran down the slope.

The triggering times and respective precipitation amount and intensity are shown in Fig. 6. Figure 7 shows the model results together with the outline of the actually affected areas, which show good agreement. A similar validation was performed for the 2000 and 2002 events, as seen on Fig. 7.

Quantitative risk analysis

After validating the results of the debris flows models for the historical damage sites, the models were applied to the potential debris flow sites indicated in Fig. 3. The results were subsequently used in combination with building information for the quantification of potential damage to buildings and people for three return periods using two vulnerability curves (for depths and impact pressures, respectively) proposed by Quan Luna et al. (2011). Direct losses to the buildings were calculated by multiplying the calculated vulnerability by the building value (Fig. 8).

Fig. 6 Total rainfall amount and intensity from May 1983, which lead to triggering of three large debris flows. Triggering times of the flows are shown by the arrows; *M* middle flow, *E* eastern flow, *W* western flow

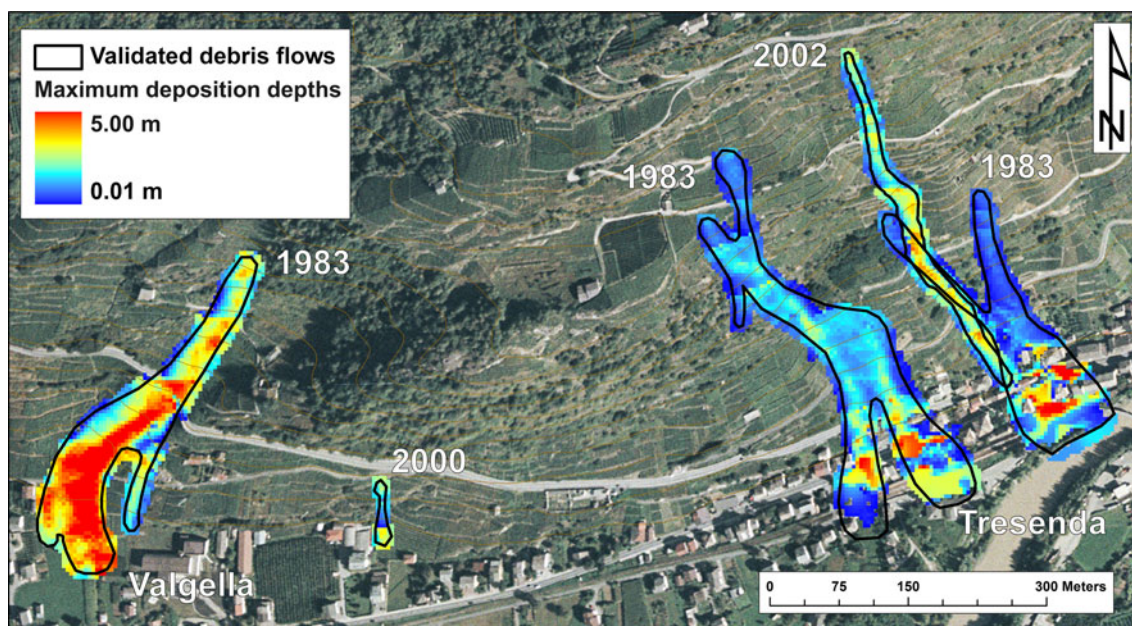
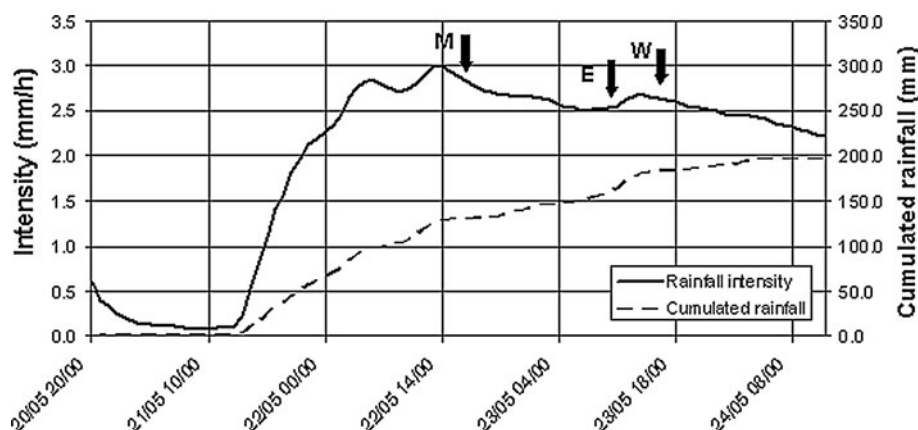


Fig. 7 Results from the validation of the 1983, 2000 and 2002 debris flows modelled with geotechnical parameters similar to those used in the hazard scenario preparation. The *solid black line* represents the

real extent of the debris flows, while the *coloured raster* shows the modelled results

Individual risk to life of people in the buildings was also assessed.

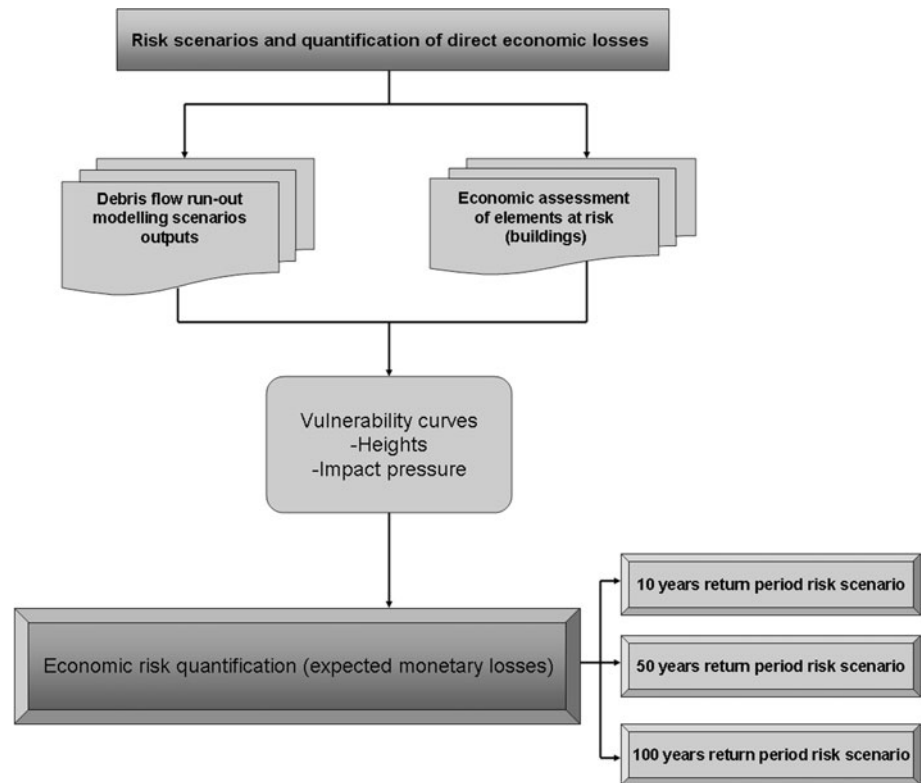
Elements at risk in the study area

A total of 111 buildings were mapped in Tresenda, 57 of which are located in areas that might be affected by the potential debris flows. The majority consists of two/three-storey reinforced concrete frame buildings with brick masonry walls. The value of each building was estimated using the construction prices provided by the association of engineers and architects from Milan (DEI 2006). According to them, a construction cost of 801 €/m² corresponds to a single 2–3 storey standing house. The value of the

buildings was calculated by multiplying their footprint area from the DB2000 (2003) database by the number of floors and by the reconstruction value per m². The total value of the potentially exposed buildings is almost 14.9 million € with values of individual buildings ranging between 0.034 and 1.1 million with an average value of 0.26 million.

Beside the buildings, the state road S.S.38 is located in the potentially affected area between the buildings and the Adda River and minor paved roads are also within the run-out zone. A principal railway line is running along the state road, connecting the provincial capital of Sondrio with Tirano and Switzerland, upstream of the Adda River. According to the database of the registry office, 173 people are living in the houses within the delimited study area.

Fig. 8 Flowchart of the methodological framework for the debris flow risk scenario assessment



Hazard scenarios and damage to buildings and people

A total of six hazard scenarios for the three return periods were prepared. For each return period two maps were generated with deposition depths and impact pressures, respectively. The results are presented in Fig. 9 in which also the possible damage to the buildings is shown, resulting from the calculated vulnerability using two types of vulnerability functions: on the left for deposition depth and on the right for impact pressure, obtained from Quan Luna et al. (2011) (Fig. 10). Light damage means vulnerability between 0 and 0.1, medium damage represents vulnerability from 0.2 to 0.4 and heavy damage relates to vulnerabilities between 0.5 and 0.9. Destruction means that vulnerability of one was reached. The vulnerability curves used and presented in this study were derived from a case that happened in a nearby area (Selvetta case study). This was done because of limited data available for this study area and the similarity in the type of buildings. In addition, very limited damage data and vulnerability functions can be found for debris flows in general. However, we believe that the used functions are transferable to other Italian Alpine regions and to the area of Valtellina Valley which is very conservative in terms of building types, construction and materials used. Older buildings in the area are made from stone/brick masonry usually having two or three floors. The buildings in Tresenda (except of those rebuilt after the 1983 event) are the older ones, at least

30–40 years old. Similar buildings were affected in Selvetta (vulnerability function estimation).

This lack of data, concerning past events in the study area, restrains enormously the possibility to perform a quantitative predictive analysis of human losses. The local Registry Office suggests 273 people living in the scenario in 57 buildings potentially affected by debris flows. Based on the few historical records available and the outcomes from the hazard modelling phase, a correlation among the level of physical and human vulnerability has been attempted. The relation has been established following qualitative criteria due to the lack of data concerning the time of occupancy in relation to the period of the day in which the event might occur (temporal probability). At the same time, we assume that sudden events may happen so that early warning systems and contingency plans cannot perform efficiently (worst-case scenario). On the other hand, the number of people living in each building at risk is available as well as data concerning their age and their physical status. For a light loss to buildings (vulnerability between 0.0 and 0.1) we assume no injury to people. For a medium degree of loss to buildings (vulnerability from 0.2 to 0.4) we assume light to medium injury of people. For a heavy damage to buildings (vulnerability 0.5–0.9) we expect sever injury or life lost, and for a building destruction we expect a life lost.

This approach suggests that, if the level of the physical loss is negligible or very low and only aesthetic damage

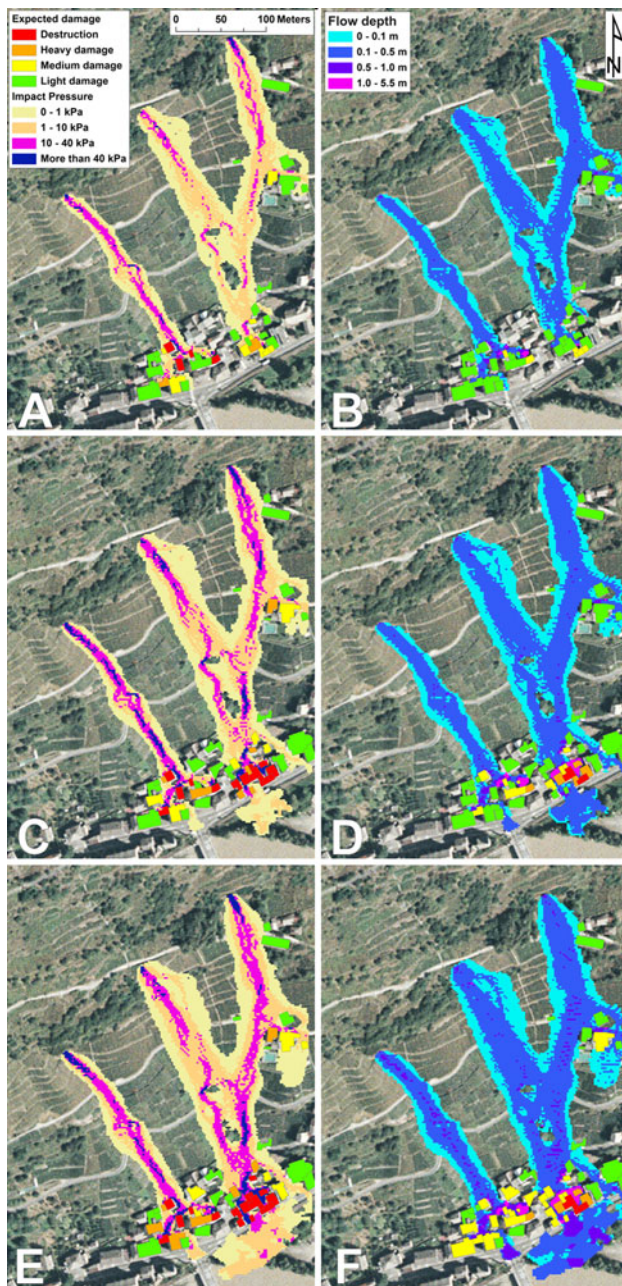


Fig. 9 Results of the 10, 50 and 100-year return period hazard modelling showing the calculated degree of damage to the buildings. On the *left* of the figure the modelled impact pressures of the flow are shown (a 10-year return period, c 50-year return period, e 100-year return period) and on the *right* of the figure the modelled flow depth are shown (b 10-year return period, d 50-year return period, f 100-year return period)

might be expected, also the level of human loss will be assumed to be very low or null. By increasing the level of physical loss, so that functional damage is supposed, the expected human loss might increase from light to medium level of injury, accordingly. By further increasing the level of physical loss, so that structural damage to complete destruction of the buildings might be expected, the level of

human loss rises consequently and casualties might be assumed.

An advantage of the applied methodology is that it can be updated with different types of vulnerability functions and/or fragility curves. Nevertheless, the presented vulnerability functions do not conflict with the damage state probability functions that plot probabilities of the different damage states of a structure (e.g. slight damage, moderate damage, complete collapse). Whereas in the damage stage functions the proposed stage ranges are determined qualitatively in a subjective manner and the probability of complete collapse can be smaller than one, in the proposed vulnerability curves the degree of damage is determined directly by the intensity of the event and a complete collapse takes a value of one. For this reason, the values determined by the vulnerability functions can be used directly in a quantitative risk assessment (Quan Luna et al. 2011). Similarly, the proposed correlation between physical and human vulnerability can be improved when more reliable data will be available.

Risk scenarios and quantification of direct economic and human loss

10-year return period

In the 10-year return period hazard scenario (0.1 annual probability) of the debris flows, 35 buildings are likely to be impacted. After the application of the vulnerability function based on the deposition depth, 30 buildings would suffer light damage and 5 buildings medium damage. None of the buildings would be destroyed or suffer heavy structural damage. After application of the impact pressure vulnerability function, a very different risk pattern appears: 19 buildings would suffer light damage, 10 buildings would have medium damage and 2 buildings would be heavily damaged. Four buildings are likely to be destroyed in this scenario. Since these results are very different the question about the appropriate vulnerability function arises. The total direct damage to houses is considerably affected by the use of different vulnerability functions. Considering the depth vulnerability function, the direct damage reaches 5,61,000 €. In the case of impact pressure vulnerability function, the total direct monetary loss to the buildings is estimated to 19,96,000 € (356 % of the first damage estimate). Risk levels span from 0 (no risk) to almost 9,000 €/year for a single building in case of the depth of deposition vulnerability function and from 0 to almost 28,000 €/year for a single building in case of the use of impact pressure vulnerability function (Fig. 11). Concerning the human loss perspective, 96 people are expected to suffer no harm while 16 might support light to medium injury; no people are expected to suffer severe injury to death in the 10-year

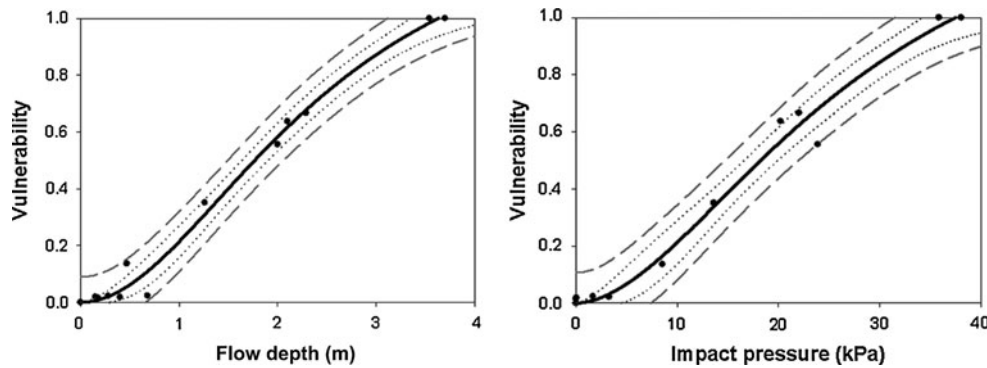


Fig. 10 Vulnerability functions used for the economic debris flow risk assessment obtained from Quan Luna et al. (2011). The *black line* corresponds to the vulnerability function; the *dotted line* represents the 95 % confidence band and the *hyphenated line* denotes the 95 %

return period scenario based on the deposition depth vulnerability function. If the impact pressure vulnerability function is applied, then the number of people not affected by the event decreases to 61; light to medium injury might affect 28 people, 7 people could support severe injury to possible death and 13 people might lose their life.

50-year return period

In the 50-year return period hazard scenario (0.02 annual probability), 49 buildings are likely to be impacted. After the application of the vulnerability function using as an intensity parameter the deposition depth, 19 buildings would suffer light damage, 22 buildings medium damage, and 4 buildings high damage. Four buildings would be completely destroyed. After application of the impact pressure vulnerability function: 17 buildings would suffer light damage, 6 buildings would have medium damage and 8 buildings would have heavy damage. Eighteen buildings would be destroyed. These results show the same pattern as in the case of 10 and 50-year return periods. The number of affected houses is similar to the previous scenario. Expected damage is, however, much higher. The total direct damage to houses is considerably affected by the use of the different vulnerability functions as in the case of the previous scenarios. Considering the deposition depth vulnerability function, the direct damage reaches 22,41,000 €. In the case of impact pressure vulnerability function, it reaches 50,45,000 €. This is 225 % of the first damage estimate. Risk reaches almost 8,000 €/year for a single building in both cases of risk calculation (Fig. 11). From the human loss point of view, in the 50-year return period scenario, based on the depth of deposition vulnerability function, 101 people are predicted to suffer no injury while 24 might suffer light to medium injury, 16 from severe injury to possible death and 10 might die. The number of people not affected by the event decreases to 65 if the impact pressure vulnerability function

prediction band. The curves were calculated in the context of physical vulnerability, which was calculated as the ratio between the monetary loss and the reconstruction value based on the Selvetta debris flow event of 2008 (inside the Valtellina valley)

is applied; light to medium injury might endanger 23 people, 19 people could support severe injury to possible death while 47 people might lose their life.

100-year return period

In the 100-year return period hazard scenario (0.01 annual probability), 49 buildings are likely to be impacted as in the case of the 50-year scenario. After the application of the vulnerability function using as an intensity parameter the deposition depth, 19 buildings would suffer light damage, 22 buildings medium damage, and 4 buildings high damage. Four buildings would be completely destroyed. After application of the impact pressure vulnerability function: 17 buildings would suffer light damage, 6 buildings would have medium damage and 8 buildings would have heavy damage. Eighteen buildings would be destroyed. These results show the same pattern as in the case of 10 and 50-year return periods. The number of affected houses is similar to the previous scenario. Expected damage is, however, much higher. The total direct damage to houses is considerably affected by the use of the different vulnerability functions as in the case of the previous scenarios. Considering the deposition depth vulnerability function, the direct damage reaches 31,06,000 €. In the case of impact pressure vulnerability function application, the total direct monetary loss to the buildings is estimated to 63,68,000 € (205 %). This estimate is only two times higher than in the case of deposition depth vulnerability function (much lower than in previous 10 and 50-year return period scenarios). Risk reaches almost 4,000 €/year for a single building in case of the deposition depths vulnerability calculation and 6,000 €/year for a single building in case of the impact pressure use (Fig. 11). In the 100-year return period scenario, 59 people are expected to suffer no injury while 68 might support light to medium injury, 14 from severe injury to possible death and 13 people might die if the deposition depth vulnerability function is

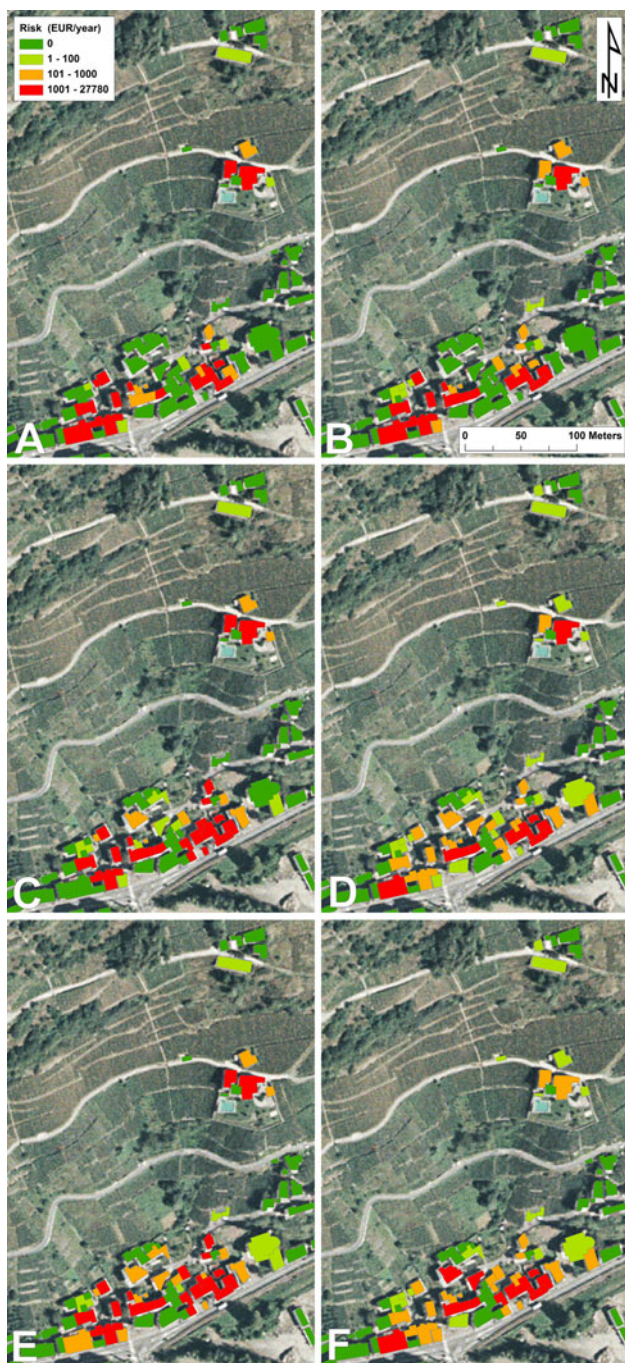


Fig. 11 Debris flows risk maps for a 10, 50 and 100-year return period. On the *left* of the figure the modelled impact pressures of the flow are shown (a 10-year return period, c 50-year return period, e 100-year return period) and on the *right* of the figure the modelled flow depths are shown (b 10-year return period, d 50-year return period, f 100-year return period)

considered. If the impact pressure vulnerability function is applied, then the number of people expected to suffer no harm decreases to 54; light to medium injury might involve 17 people, 26 people could support severe injury to possible death while 61 people might lose their life.

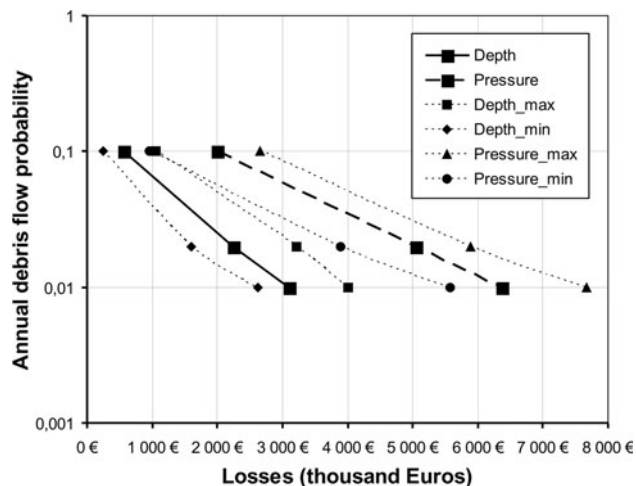


Fig. 12 Debris flows risk curves calculated for the two different vulnerability curves with their maximum and minimum ranges. The range variation accounts for the uncertainty in the run-out modelling parameters and the vulnerability curves

A quantitative risk assessment should account for the in the analysis uncertainties where possible and express them as a range of risk values. These estimations should also be included in the analysis. Considering the impact of the uncertainties in this analysis, an evaluation for each scenario proposed (10, 50 and 100-years return periods) was implemented. This evaluation incorporated the variation of the input parameters used for the run-out modelling based on the variation of the laboratory analysis results and the application of the 95 % confidence intervals of the proposed vulnerability curves. Maximum and minimum values of the laboratory analysis were used and varied as inputs inside the run-out assessment of the hazard (Table 2). This variation to the modelled run-out, influenced the spatial distribution of the flow as well as the deposition depths and the impact pressures outputs. The resulting values of the modelled run-out were applied to the 95 % confidence intervals of the vulnerability curves to compute the economic risk of each variation. Moreover, 95 % confidence interval was applied also to the construction unit price of the buildings. As a result, three curves of expected losses were obtained for each flow vulnerability attribute: maximum, average and minimum risk curve for the accumulation of the flow and maximum, average and minimum risk curve for the estimated impact pressure (Fig. 12).

Discussion and conclusions

Six risk scenarios were compared (for the three return periods and for the two vulnerability functions each). The results are summarised in Table 5. There are, however, considerable differences between the estimates for the

Table 5 Summary of the economic losses and the differences between the application of the different types of vulnerability curves

Damage	Vulnerability	10-year return period		50-year return period		100-year return period	
		Nr_B D.D.	NR_B I.P.	Nr_B D.D.	NR_B I.P.	Nr_B D.D.	NR_B I.P.
Light	0–0.1	30	19	32	21	19	17
Medium	0.2–0.5	5	10	9	7	22	6
Heavy	0.6–0.9	0	2	5	7	4	8
Destruction	1	0	4	3	14	4	18
Losses (million €)		0.56	2.00	2.24	5.05	3.11	6.37

Nr_B number of buildings affected, *D.D.* deposition depth, *I.P.* impact pressure

same return periods. Usage of the impact pressure vulnerability curve gives substantially higher estimates than the application of deposition depth vulnerability function. This difference is, however, decreasing with the increasing magnitude/volume of the debris flows. The results show that high difference between the two vulnerability curves applied arises when they are used for the prospective damage estimation (Fig. 13). In an ideal case, the comparison between the curves would make a straight line going from 0 to 1. However, the scatter cloud shows the differences for each potentially affected building.

The main objective of the comparison between the vulnerability functions of impact pressure and deposition depth was to highlight the uncertainty involved in the usage of vulnerability functions in a Quantitative Risk Assessment. The majority of available vulnerability functions for debris flows are based on the flow height/deposition depth. An exception is the work of Jakob et al. (2012) who used a

debris flow intensity index expressed as the product of the velocity squared and flow depth. The purpose of this comparison was to assess the use of other intensity parameter such as impact pressure. In our opinion, we believe the impact pressure information is more important for the assessment of the vulnerability (damage) to the buildings because as it may better estimate building damage than approaches that account only for flow depth. The vulnerability functions for impact pressure were compared to the impact pressure vulnerability functions available for snow avalanches (Quan Luna et al. 2011) and they agreed in terms of the force intensities (kPa) that the structure can or can not resist.

However, the main differences in applying vulnerability function from one place to another are not in the vulnerability function estimates but are due to the morphology of the slope, the position of the buildings on the slope and the properties of the debris flow. In the Tresenda case, the slope is very steep not allowing the flow depth to increase a lot. The majority of the buildings are situated directly on the steep slopes, where the flow has high speed but low depth (high impact pressure) and only few buildings are situated in areas where the flow slows and deposition depths increase. We thus agree with Jakob et al. (2012) and conclude that usage of a simple flow height vulnerability curve for a QRA is not sufficient and needs to be supported with impact pressure information, which is crucial for the assessment of the stability of the buildings affected.

The debris flow modelling and hazard analysis allowed quantification of the economic risk to exposed buildings. However, some limitations and uncertainties remain which need to be addressed. First, it is assumed that the return period of a rainfall, potentially causing a debris flow, is the same as the return period of the resulting debris flow. Also, the antecedent rainfall and the related moisture conditions of soil are not taken into account in this analysis. Other assumptions arise from the modelling itself: DEM resolution, rheological properties acquired in the laboratory and upscaled to the entire area and volume estimates. Other implications related to the application of vulnerability curves applied to the Tresenda scenario which might

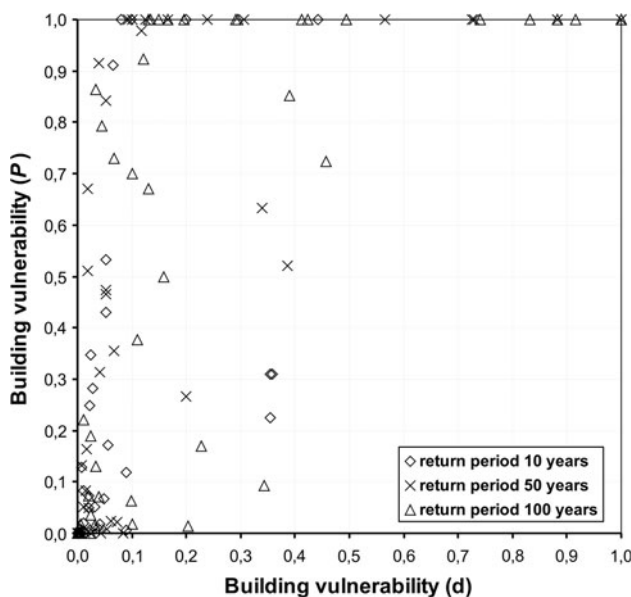


Fig. 13 Comparison of vulnerability estimates for three return periods using two vulnerability curves: impact pressure (*p*) and deposition depth (*d*)

seriously affect the resulting damage and risk estimates were already discussed. It turned out, that the use of impact pressure-based vulnerability curve is giving much higher damage estimates than the deposition depth-based vulnerability curve. Moreover, the dynamic aspect of debris flows is not ignored when the impact pressure vulnerability curve is applied. Estimated economic value of the building also affects results, as it is assumed similar unit value of buildings, neglecting its particular conditions and current state. Finally, estimates about the value of the furniture and expenses needed to remove and re-deposit the debris material, or damage to the roads and lifelines are not taken into account.

Although this study is mainly intended to assess quantitatively the economic risk to buildings, an attempt has been performed to analyze the human losses. A correlation has been attempted between the level of physical vulnerability (coming from the hazard modelling phase) and the expected human loss concerning 273 people living in the scenario into 57 buildings potentially affected by debris flows. As argued before, sudden events are considered in the analysis, so that early warning systems and contingency plans cannot perform efficiently in saving lives (worst-case scenario).

Besides the presented limitations, we believe that the approach applied in this analysis is generally applicable to other areas and may give important information to the local stakeholders. The presented approach allowed to assess debris flow hazard and risk in a quantitative way and to calculate prospective direct damage to buildings as well as human losses. Direct economic losses to the buildings were estimated, reaching 5,61,000–63,68,000 €, depending on the hazard scenario return period and vulnerability curve used. With the 95 % variation of the input parameters the loss range from 2,49,000–76,72,000 €, respectively. Concerning the human losses, in case of the complete destruction of the buildings is expected, the number of people that could lose their life increases from 0 to 13 if the deposition depth vulnerability function is applied, from 10- to 100-year return period hazard scenarios; 13–61 if the impact pressure vulnerability function is used considering the same time span.

The approach proposed in this study may assist local decision makers in determining the nature and the magnitude of the expected (physical, economic and societal) losses due to a dangerous event and may help public administrators, economic planners and lawmakers allocating financial resources for disaster prevention and for mitigation measures (Sterlacchini et al. 2007). It is obvious that the approach still has some weak points as the one regarding the assessment of people's vulnerability. In any case, also the information provided and concerning human losses can be proficiently used by disaster managers, technicians and

authorities to calibrate preparedness and response activities in the field of Civil Protection. In this way the approach proposed in this study may increase the knowledge about prospective outcomes of future hazards thus contributing to the protection of the people and their assets.

Acknowledgments The authors would like to thank the reviewers for their valuable comments, which improved the quality of the manuscript. We also thank to Dr. H. Kross and S.L. Manuela for fruitful discussions on the early versions of the manuscript. This work has been supported by the Marie Curie Research and Training Network "Mountain Risks" funded by the European Commission (2007–2010, Contract MCRTN-35098).

References

- Agliardi F, Crosta GB, Frattini P (2009) Integrating rockfall risk assessment and countermeasure design by 3D modelling techniques. *Nat Hazards Earth Syst Sci* 9:1059–1073. doi:10.5194/nhess-9-1059-2009
- Agostoni S, Laffi R, Sciesa E (1997) Centri abitati instabili della provincia di Sondrio. CNR-GNDICI, Milan, p 59
- Azzola M, Tuia T (1983) Osservazione sui fenomeni franosi che hanno interessato i vigneti terrazzati a monte di Tresenda nel maggio 1983. *Geol Tec* 4:23–35
- Bell R, Glade T (2004) Quantitative risk analysis for landslides—examples from BÍldudalur, NW-Iceland. *Nat Hazards Earth Syst Sci* 4:117–131. doi:10.5194/nhess-4-117-2004
- Blahut J, van Westen CJ, Sterlacchini S (2010) Analysis of landslide inventories for accurate prediction of debris-flow source areas. *Geomorphology* 119(1–2):36–51. doi:10.1016/j.geomorph.2010.02.017
- Blahut J, Poretti I, De Amicis M, Sterlacchini S (2012) Database of geo-hydrological disasters for civil protection purposes. *Nat Hazard* 60(3):1065–1083. doi:10.1007/s11069-011-9893-6
- Blahut J, Klimeš J, Vařilová Z (2013) Quantitative rockfall hazard and risk analysis in selected municipalities of the České Švýcarsko national park, northwestern Czechia. *Geografie* 118(3):205–220
- Camera C, Apuani T, Masetti M (2012a) Mechanisms of failure on terraced slopes: the Valtellina case (northern Italy). *Landslides Online First*. doi:10.1007/s10346-012-0371-3
- Camera C, Masetti M, Apuani T (2012b) Rainfall, infiltration, and groundwater flow in a terraced slope of Valtellina (northern Italy): field data and modelling. *Environ Earth Sci* 65(4):1191–1202. doi:10.1007/s12665-011-1367-3
- Cancelli A, Nova R (1985) Landslides in soil debris cover triggered by rainstorms in Valtellina (Central Alps—Italy). In: Proceedings of 4th international conference and field workshop on landslides, The Japan Geological Society, Tokyo, pp 267–272
- Cascini L, Bonnard Ch, Corominas J, Jibson R, Montero-Olarte J (2005) Landslide hazard and risk zoning for urban planning and development. In: Balkema (ed) Proceedings of the international conference on landslide risk management, Vancouver, 31 May–3 June 2005, pp 199–235
- Castellanos AEA (2008) Local landslide risk assessment. In: Castellanos AEA Multi-scale landslide risk assessment in Cuba. ITC Dissertation, Utrecht University, Utrecht
- Ceriani M, Lauzi S, Padovan N (1992) Rainfall and landslides in the Alpine area of Lombardia Region, Central Alps, Italy. In: Proceedings of the Internationales Symposium Interpraevent, Bern 2:9–20

- Chang TC, Wang ZY, Chien YH (2010) Hazard assessment model for debris flow prediction. *Environ Earth Sci* 60(8):1619–1630. doi:10.1007/s12665-009-0296-x
- Corominas J, Mavrouli O (2011) Quantitative risk assessment for buildings due to rockfalls: some achievements and challenges. In: *Journée de Rencontre sur les Dangers Naturels. "2ème Journée de Rencontre sur les Dangers Naturels 2011"*, Lausanne, p 1–8
- Crosta GB, Dal Negro P, Frattini P (2003) Soil slips and debris flows on terraced slopes. *Nat Hazards Earth Syst Sci* 3:31–42. doi:10.5194/nhess-3-31-2003
- Crosta GB, Frattini P, Fugazza F, Caluzzi L, Chen J (2005) Cost-benefit analysis for debris avalanche risk management. In: Hungr O, Fell R, Couture R, Eberhardt E (eds) *Landslide risk management*. Taylor & Francis, London, pp 533–541
- Cruden D, Fell R (1997) *Landslide risk assessment*. Proceedings of the international workshop on landslide risk, Honolulu, USA, Feb 1997
- Dai FC, Lee CF, Ngai YY (2002) Landslide risk assessment and management: an overview. *Eng Geol* 64(1):65–87. doi:10.1016/S0013-7952(01)00093-X
- DB2000 (2003) Database of the CM Valtellina di Tirano mapped at 1:2,000 scale. CM Valtellina di Tirano. CD-ROM. Available at: <http://www.cmtirano.so.it/sistemainformativo.php>
- DEI (2006) *Prezzi Tipologie Edilizie 2006*. DEI Tipografia del Genio Civile. CD-ROM
- FLO-2D (2009) Reference manual 2009. FLO-2D Software Inc., p 73. Available at: <http://www.flo-2d.com/wp-content/uploads/FLO-2D-Reference-Manual-2009.pdf>
- Fuchs S, Kaitna R, Scheidl C, Hübl J (2008) The application of the risk concept to debris flow hazards. *Geomech Tunn* 1(2):120–129
- Giacomelli L (1987) *Speciale Valtellina 1987: Cronaca, storia, commenti*. Notiziario della Banca Popolare di Sondrio, No. 45, Bergamo, p 227
- Glade T, Anderson M, Crozier MJ (eds) (2005) *Landslide hazard and risk*. John Wiley, Chichester
- Govi M, Mortara G, Sorzana P (1984) *Eventi idrologici e frane*. Geologia Applicata e Idrogeologia, XCVIII, p 3
- Gumbel EJ (ed) (2004) *Statistics of extremes*. Reprint of the 1958 edition. Dover, Mineola
- Guzzetti F, Crosta G, Marchetti M, Reichenbach P (1992) Debris flows triggered by the July, 17–19, 1987 storm in the Valtellina area (northern Italy). In: *International symposium interpraevent*, Bern, Switzerland, 1992, pp 193–203
- Guzzetti F, Reichenbach P, Ghigi S (2004) Rockfall hazard and risk assessment in the Nera River Valley, Umbria Region, Central Italy. *Environ Manag* 34(2):191–208. doi:10.1007/s00267-003-0021-6
- Hürlimann M, Copons R, Altimir J (2006) Detailed debris flow hazard assessment in Andorra: a multidisciplinary approach. *Geomorphology* 78:359–372. doi:10.1016/j.geomorph.2006.02.003
- Jaiswal P, van Westen CJ, Jetten V (2010) Quantitative landslide hazard assessment along a transportation corridor in southern India. *Eng Geol* 116(3–4):236–250. doi:10.1016/j.enggeo.2010.09.005
- Jakob M, Stein D, Ulmi M (2012) Vulnerability of buildings to debris flow impact. *Nat Hazard* 60:241–251. doi:10.1007/s11069-011-0007
- Khan YA, Lateh H, Baten MA, Kamil AA (2012) Critical antecedent rainfall conditions for shallow landslides in Chittagong City of Bangladesh. *Environ Earth Sci* 60(8):1619–1630. doi:10.1007/s12665-011-1483-0
- Lara M, Sepulveda SA (2010) Landslide susceptibility and hazard assessment in San Ramn Ravine, Santiago de Chile, from an engineering geological approach. *Environ Earth Sci* 67(1):97–106. doi:10.1007/s12665-009-0264-5
- Leroi E, Bonnard Ch, Fell R, McInnes R (2005) A framework for landslide risk assessment and management. In: Hungr O, Fell R, Couture R, Eberhardt E (eds) *Landslide risk management*. Taylor & Francis, London, pp 159–198
- Li Z, Huang H, Nadim F, Xue Y (2010) Quantitative risk assessment of cut-slope projects under construction. *J Geotech Geoenviron Eng*. doi:10.1061/(ASCE)GT.1943-5606.0000381
- Luino F, Nigrelli G, Biddoccu M, Cirio CG, Di Palma M, Missaglia M, Fassi P (2008) Definizione delle soglie pluviometriche d'innescio di frane superficiali e colate torrentizie: accorpamento per aree omogenee. IRER, Milano, p 125
- Malet J-P, Laigle D, Remaître A, Maquaire O (2005) Triggering conditions and mobility of debris-flows associated to complex earthflows. *Geomorphology* 66(1–4):215–235. doi:10.1016/j.geomorph.2004.09.014
- Michael-Leiba M, Baynes F, Scott G, Granger K (2003) Regional landslide risk to the Cairns community. *Nat Hazard* 30(2):233–249. doi:10.1023/A:1026122518661
- Muir I, Ho KSS, Sun HW, Hui THH, Koo YC (2006) Quantitative risk assessment as applied to natural terrain landslide hazard management in a mid-levels catchment, Hong Kong. In: Nadim F, Pottler R, Einstein H, Klapperich H, Kramer S (eds) "Geohazards", ECI Symposium Series, P07, p 8
- O'Brien JS, Julien PY (1988) Laboratory analysis of mudflow properties. *J Hydraul Eng* 114(8):877–887. doi:10.1061/(ASCE)0733-9429
- Quan Luna B, Blahut J, van Westen CJ, Sterlacchini S, van Asch TWJ, Akbas SO (2011) The application of numerical debris flow modelling for the generation of physical vulnerability curves. *Nat Hazards Earth Syst Sci* 11:2047–2060. doi:10.5194/nhess-11-2047-2011 2011
- Remondo J, Bonachea J, Cendrero A (2008) Quantitative landslide risk assessment and mapping on the basis of recent occurrences. *Geomorphology* 94(3–4):496–507. doi:10.1016/j.geomorph.2006.10.041
- Sterlacchini S, Frigerio S, Giacomelli P, Brambilla M (2007) Landslide risk analysis: a multi-disciplinary methodological approach. *Nat Hazards Earth Syst Sci* 7:657–675. doi:10.5194/nhess-7-657-2007
- van Westen CJ, van Asch TWJ, Soeters R (2006) Landslide hazard and risk zonation—why is it still so difficult? *Bull Eng Geol Environ* 65:167–184. doi:10.1007/s10064-005-0023-0
- Wong HN, Ko FWY (2005) *Landslide risk assessment—application and practice (SPR 4/2005)*. Geotechnical Engineering Office, Hong Kong, p 311
- Zêzere JL, Garcia RAC, Oliveira SC, Reis E (2008) Probabilistic landslide risk analysis considering direct costs in the area north of Lisbon (Portugal). *Geomorphology* 94(3–4):467–495. doi:10.1016/j.geomorph.2006.10.040